Three-Dimensional Analysis of Beamlet Deflection in a MeV Accelerator for ITER NBI

Mieko KASHIWAGI, Masaki TANIGUCHI, Naotaka UMEDA, Takatoshi MIZUNO, Hiroyuki TOBARI, Masayuki DAIRAKU, Kazuhiro WATANABE and Takashi INOUE

Japan Atomic Energy Agency (JAEA), 801-1 Mukoyama, Naka 311-0193, Japan

(Received 18 December 2009 / Accepted 4 March 2010)

At Japan Atomic Energy Agency (JAEA), a MeV accelerator has been developed to demonstrate acceleration of H^- ion beams at the ITER-relevant power density. After long pulse beam acceleration tests of up to 10 s, molten areas were observed around the apertures of the grids due to excess heat load on the grids. To identify the cause of the melting, a three-dimensional (3D) beam analysis was performed. The stripping loss of negative ions and magnetic fields in the accelerator were included in the calculation to examine the beam trajectories precisely. It was clarified that the beamlet deflection angle was larger than 10 mrad due to space charge repulsion among the beamlets and magnetic fields, which resulted in excess heat loads of more than 20 kW/cm^2 at the grounded grid. To compensate for beamlet deflections, an aperture offset and field shaping plate were designed.

Keywords: ITER, NBI, accelerator, negative ion beam, space charge, beam deflection

DOI: 10.1585/pfr.5.S2097

1. Introduction

An accelerator that generates deuterium negative ion beams of 1 MeV, at 40 A (200 A/m^2) for 3600 s is required for a neutral beam injector (NBI) for ITER [1]. As the ITER baseline accelerator, a multi-aperture, multi-grid (MAMuG) accelerator has been chosen because of its higher voltage holding capability compared to a single-aperture, single-gap (SINGAP) accelerator [2]. In the MAMuG accelerator, since multi-beamlets are accelerated through the multiple apertures, it is essential to control each beamlet precisely to suppress heat loads on the grids by beamlet deflection due to space charge repulsion among the beamlets and magnetic fields in the accelerator.

At Japan Atomic Energy Agency (JAEA), high power negative ion acceleration tests have been progressed using a MAMuG accelerator called the MeV accelerator [3], whose target is H^- ion beam acceleration of 200 A/m^2 at 1 MeV. In the original accelerator using acceleration grids without water cooling, H^- ion beams of 800 keV were achieved under perveance matched conditions for 0.2 s [4]. In long pulse tests of up to 10 s using water-cooled grids, beam acceleration succeeded for 10 s at 600 keV under perveance matched conditions and for 5 s at higher beam energies up to 800 keV but under perveance conditions [5]. After these tests, a grounded grid was found melted around the grid apertures [6].

To examine beamlet deflection and the compensation method, a three dimensional (3D) beam analysis has been conducted [2, 7]. This work was performed using the OPERA-3d code combined with a 3D Monte Carlo gas flow code and a two-dimensional (2D) beam analysis code developed in JAEA [8–10]. Taking into account stripping loss of negative ions in the accelerator, the analyzed beamlet deflection angle was in good agreement with that of experiments, suggesting deflections due to space charge repulsion and distortion of electric fields by grid supports in the original accelerator [8].

In this study, magnetic deflections were also considered in examining beamlet deflection followed by possible grid melt. In section 2, the numerical model is described. In section 3, the experimentally measured beamlet deflections are discussed. The beamlet deflections and their compensations are examined in sections 4 and 5, respectively, using 3D multi beamlet analysis.

2. Numerical Model

Figure 1 shows a cross sectional view of the calculation model, which is the MeV accelerator used in long pulse tests, called the "long pulse accelerator". For comparison, the original accelerator with five acceleration grids is shown on the left. The extractor is the same in both accelerators. Negative ions produced in the KAMABOKO source [11] are extracted by the potential difference between a plasma grid (PG) and an extraction grid (EXG) through fifteen apertures drilled in a lattice pattern of 5 rows × 3 columns. Dipole magnetic fields are generated by magnets embedded in the EXG for electron suppression. An electron suppression grid (ESG) is attached to the back of the EXG to trap the electrons deflected by the magnetic field. This magnetic field also deflects the H^- ion beam itself in $\pm x$ direction alternatively in each row. In

author's e-mail: kashiwagi.mieko@jaea.go.jp

addition, transverse magnetic fields called filter fields are generated in the x direction by filter magnets embedded in the KAMABOKO source. This field causes magnetic deflection of the beamlets in the y direction. The accelerator was modified for long pulse tests as follows.

i) Addition of water-cooled acceleration grids
ii) Removal of second acceleration grid (called A2G) to simplify the accelerator.
iii) Grid modification from thick grids to thinner grid having tapered apertures with electron traps for electron suppression [Fig. 1 (b)].

The accelerator comprises three intermediate grids called A1G, A3G, and A4G, and a grounded grid (GRG). The aperture diameter is decreased from 16 mm in the original to 14 mm to accommodate water channels. These grids are made of oxygen-free copper. The original accelerator had a 50 mm wide gap between the grid supports and the fiberglass-reinforced plastic (FRP) insulator column, which was effective for gas pumping. To maintain the gas conductance in the long pulse accelerator, several large openings were provided in the grid support flanges as substitute for the gas pumping path.

In the 3D beam analysis, the OPERA-3d code for calculating multiple beamlets was combined with JAEA codes, a 3D Monte Carlo gas flow code for calculating the stripping loss of negative ions and a 2D beam analysis

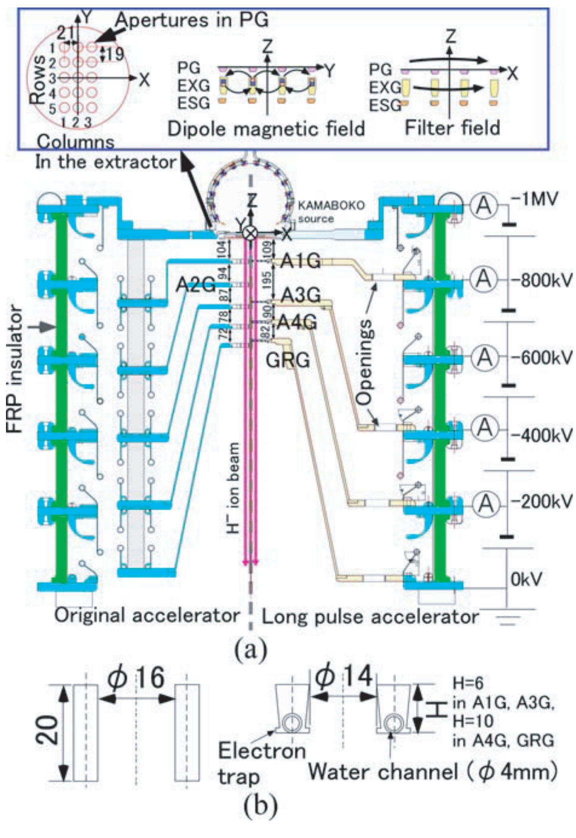

Fig. 1 Calculation model: Cross sections of (a) accelerators and (b) apertures in acceleration grids, in the original (left) and long pulse (right) accelerators.

code, BEAMORBT, for calculating the beam initial parameters as input data in the OPERA-3d code. The permanent magnets ($5.4 \times 4.6\,\text{mm}^2$ in cross section) in the ESG and those in the KAMABOKO source [11] for the magnetic filter were modeled with their residual magnetic flux density of 0.9 T.

In the 3D gas flow code, the gas pressures in the KAMABOKO source and in the accelerator downstream were 0.19 Pa and 0.1 Pa, respectively. These values correspond to the measured ones and are almost the same as those in the original accelerator. The stripping loss was estimated to be 37% at a beam energy of 600 keV.

In the 2D BEAMORBT code, the beam conditions for achieving the minimum beam divergence angle were in good agreement with the experimental ones [8]. However, the absolute value of the beam divergence angle in the calculation was smaller than that in the measurement. This is partly because ions extracted within a distance of 0.1 mm from the aperture edge in the PG were neglected in the analyses to better represent the core beams rather than beam aberration components formed by the ions extracted from the edge region of the aperture and then accelerated in fringe fields. The 3D beam analyses also represent the core beams.

3. Experimental Beamlet Deflection

Figure 2 shows photographs of the grid surfaces for (a) A1G and (b) GRG taken after the long pulse tests. Outlines of beam footprints on A1G are traced by dotted circles. The beam footprints were displaced in the $\pm x$ direction alternately in each row. These directions correspond to beamlet deflection due to the alternating dipole magnetic field. The displacement distance from aperture centers to beam centers is shown in Fig. 2 (a). The displacement distances were about 1.8-1.9 mm in $-x$ direction in the second and forth rows and 0.2-0.5 mm in the $+x$ direction in the first, third and fifth rows. It seems that all the beamlets were deflected in the $-x$ direction. On the GRG, the molten

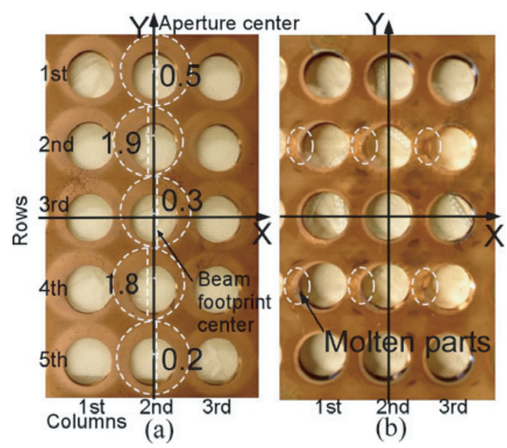

Fig. 2 Beam footprints on (a) A1G and (b) GRG.

marks were found at the edges of the aperture in the second and forth rows, as indicated by dotted circles in Fig. 2 (b). Beamlet deflection in the $-x$ direction and subsequent grid melting was also significant on the GRG. After the tests, an inclination of about 2 mrad was found in the PG due to misassembly of the grid. The beamlet deflection direction due to this inclination was also in the $-x$ direction. This could cause lower heat loads in the first, third, fifth rows and higher heat loads in the second and forth rows.

4. Numerical Study of Beamlet Deflection

Before the long pulse test, the beam optics was examined using the 2D BEAMORBT code. Figure 3 shows the beam trajectories at the minimum divergence angle in the original (a) and the long pulse (b) accelerators. In both accelerators, the beam conditions were the same: an H^- ion current density of 140 A/m^2 at the PG and extraction and acceleration voltages of 4.4 kV and 600 kV, respectively. The calculated beam divergence angle was 3 mrad. This beam condition corresponds to the optimum perveance measured in the original accelerator [4,8]. Thus, the difference between the original and long pulse accelerators was found to be negligible in the beam optics in the single beamlet analysis.

Figure 4 shows 15 beamlets in the long pulse accelerator calculated in the 3D beamlet analyses. The initial parameters obtained in Fig. 3 (b) were applied as input data. One beamlet consisted of about 700 beam particles, which is enough to calculate the space charge repulsion [2].

Figure 5 shows the distribution of heat load on the GRG surface position when the magnetic fields were (a) not included and (b) included. Fifteen circles represent the apertures, which were 14 mm in diameter. In Fig. 5 (a), the beamlets were deflected only by space charge repulsion. The largest deflection angle was 6 mrad in the x direction and 3 mrad in the y direction in peripheral beamlets. No beamlets were intercepted by the grid. When the magnetic fields were applied [Fig. 5 (b)], an additional beamlet deflection angle of 5 mrad was added in the $\pm x$ direction due to the dipole magnetic field and 3 mrad in the $+y$ direction was added owing to the filter field. When the beamlet repulsion and the magnetic deflection were opposite in the x direction, the deflection angle became small (1 mrad). In contrast, if they occurred in the same directions, the resulting beamlet deflection angle became 11 mrad. The calculated heat load due to this large deflection was 20 kW/cm^2 around the apertures. This heat load is larger than the heat removal capability of this water-cooled grid [6]. It was found that the grid melts were caused by a large beamlet deflection of more than 10 mrad even under perveance matched conditions. The heat load at the same position on A3G was 10 kW/cm^2. This is twice as high as that on the A4G. As indicated in analyses of secondary particles [12], the absence of A2G could cause concentrations of heat

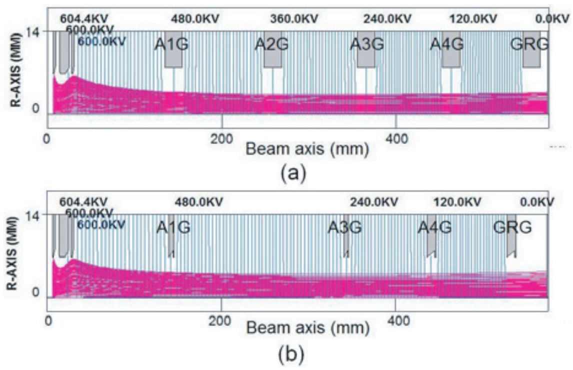

Fig. 3 2D beam trajectories at 600 keV in (a) original and (b) long pulse accelerators.

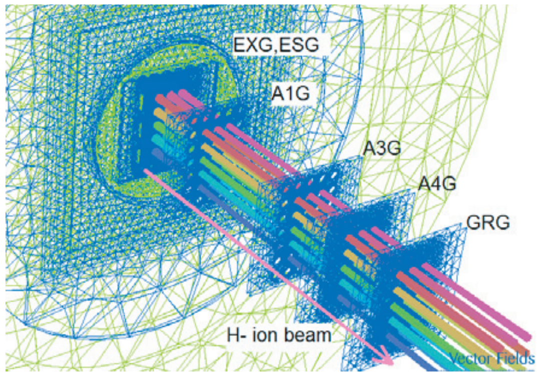

Fig. 4 Fifteen beamlets in the accelerator.

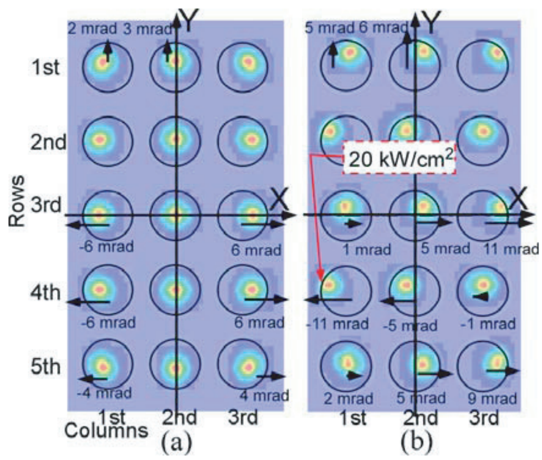

Fig. 5 Calculated beam heat loads on the GRG. Magnetic field is (a) not included and (b) included.

load on the A3G. The A2G is necessary for distribution of the heat load in each acceleration stage.

5. Compensations of Beamlet Deflection

The 3D beamlet analyses were conducted so as to compensate for beamlet deflections in the x direction. Figure 6 shows a cross sectional view of the extractor in the

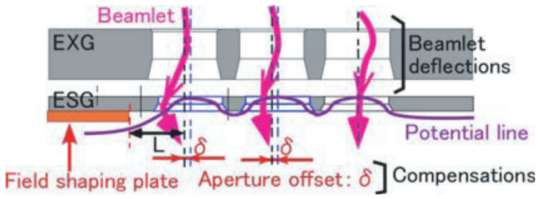

Fig. 6 Compensations for beamlet deflection.

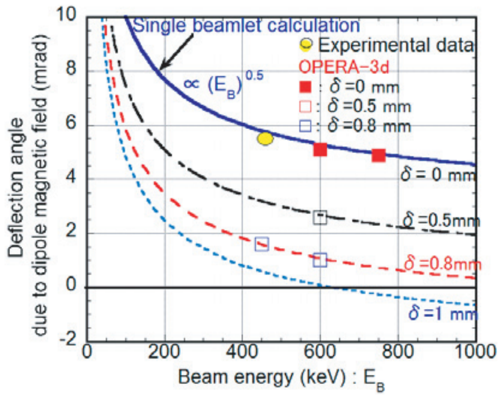

Fig. 7 Magnetic deflection before and after applying aperture offset.

second and forth rows in Fig. 5 (b). The beamlet deflection is also illustrated. Beamlet deflection is compensated for using an aperture offset in the ESG [7, 13]. The displacement distance in aperture offset should be at most 1.0 mm because large displacement of aperture may cause beam aberration and further beamlet interception at the ESG. As additional compensation for the peripheral beamlets, a-1mm-high field-shaping plate [14] is added on the back of the ESG. This generates electric field distortion that deflects the beamlet inward.

Figure 7 shows the beamlet deflection angle due to the dipole magnetic field as a function of beam energy. The bold line represents the calculated deflection angle of a single beamlet starting from the aperture center of the PG. If the beamlet is steered by the aperture offset according to thin lens theory [8, 13], the bold line is shifted to the dotted lines by aperture offsets δ of 0.5, 0.8 and 1.0 mm. The circle shows the experimental data [15]. The squares show numerical results obtained in the 3D beamlet analyses. These are in good agreement with the dotted lines corresponding to the thin lens theory. To compensate for beamlet deflections due to a dipole magnetic field of more than 600 keV, an aperture offset of 0.8 mm is necessary. However, the beamlet deflection due to space charge repulsion remained at 6 mrad, as clarified in Fig. 5 (a).

Figure 8 shows the beamlet steering angle due to the field-shaping plate as a function of distance L, between the center of the peripheral aperture and the field-shaping plate. To compensate for a beamlet deflection of 6 mrad, L should be 12 mm.

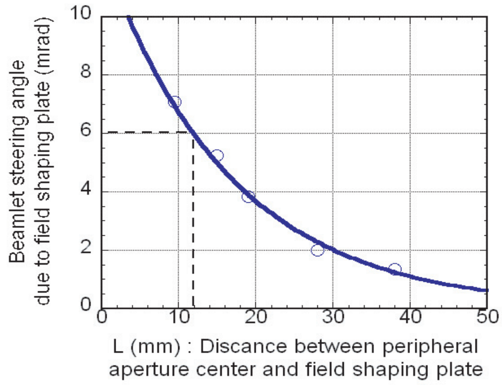

Fig. 8 Beamlet steering angle due to the field-shaping plate.

6. Summary

The 3D beam analysis showed that the beamlet deflection was more than 10 mrad due to space charge repulsion and the dipole magnetic field, and caused excess heat loads that caused melting at the GRG. This analysis also clarified that aperture offset and a field-shaping plate could compensate for the beamlet deflection precisely, which is applicable to control of each beamlet trajectory in the ITER accelerator.

For the next long pulse tests, compensation for beamlet deflection using an aperture offset of about 0.8 mm in the ESG and a field-shaping plate will be applied. In addition, new acceleration grids, including A2G, have been installed to achieve greater heat removal capability [6]. Precise alignment of the gap length between the PG and the EXG has been achieved within an accuracy of 0.1 mm.

[1] ITER EDA Final Design Report, ITER technical basis, Plant Description Document (PDD), G A0 FDR 1 01-07-13 R1.0, IAEA EDA doc. No. 24 (2002).
[2] M. Kashiwagi *et al.*, Nucl. Fusion **49**, 065008 (2009).
[3] T. Inoue, JAERI-Tech 94-007 (1994).
[4] M. Taniguchi *et al.*, Rev. Sci. Instrum. **79**, 02C110 (2008).
[5] M. Taniguchi *et al.*, Rev. Sci. Instrum. **81**, 02B101 (2010).
[6] N. Umeda *et al.*, J. Plasma Fusion Res. **9**, 259 (2010).
[7] M. Kashiwagi *et al.*, AIP conference proceedings **1097**, 421 (2008).
[8] M. Kashiwagi *et al.*, Rev. Sci. Instrum. **81**, 02B113 (2010).
[9] Cobham Technical Service Co. Ltd., Vector Fields software, http://www.vectorfields.com/.
[10] Y. Ohara, JAERI-M6757 (1976).
[11] T. Inoue *et al.*, Rev. Sci. Instrum. **75**, 1819 (2004).
[12] T. Mizuno *et al.*, Rev. Sci. Instrum. **81**, 02B103 (2010).
[13] T. Inoue *et al.*, JAERI-Tech 2000-023 (2000).
[14] M. Kamada *et al.*, Rev. Sci. Instrum. **79**, 02C114 (2008).
[15] H. P. L de Esch *et al.*, Fusion. Eng. Des. **84**, 669 (2009).